online data

Structural characterization of *Escherichia coli* sensor histidine kinase EnvZ: the periplasmic C-terminal core domain is critical for homodimerization

Ahmad KHORCHID*, Masayori INOUYE† and Mitsuhiko IKURA*[1]

*Division of Molecular and Structural Biology, Ontario Cancer Institute and Department of Medical Biophysics, University of Toronto, 610 University Avenue, Toronto, Ontario, Canada M5G 2M9, and †Department of Biochemistry, Robert Wood Johnson Medical School, Piscataway, NJ 08854, U.S.A.

Escherichia coli EnvZ is a membrane sensor histidine kinase that plays a pivotal role in cell adaptation to changes in extracellular osmolarity. Although the cytoplasmic histidine kinase domain of EnvZ has been extensively studied, both biochemically and structurally, little is known about the structure of its periplasmic domain, which has been implicated in the mechanism underlying its osmosensing function. In the present study, we report the biochemical and biophysical characterization of the periplasmic region of EnvZ (Ala^{38}–Arg^{162}). This region was found to form a dimer in solution, and to consist of two well-defined domains: an N-terminal α-helical domain and a C-terminal core domain (Glu^{83}–Arg^{162}) containing both α-helical and β-sheet secondary structures. Our pull-down assays and analytical ultracentrifugation analysis revealed that dimerization of the periplasmic region is highly sensitive to the presence of CHAPS, but relatively insensitive to salt concentration, thus suggesting the significance of hydrophobic interactions between the homodimeric subunits. Periplasmic homodimerization is mediated predominantly by the C-terminal core domain, while a regulatory function may be attributed mainly to the N-terminal α-helical domain, whose mutations have been shown previously to produce a high-osmolarity phenotype.

Key words: bacterial signal transduction, membrane receptor, NMR, osmolarity, stress response.

INTRODUCTION

Bacterial response to environmental changes is essential for their survival. The two-component regulatory systems (also referred to as the histidyl-aspartyl phosphotransfer systems) constitute the bacterial signal transduction mechanisms involved in sensing and adapting to changes in the environment (reviewed in [1–3]). In *Escherichia coli*, the sensor histidine kinase EnvZ and its cognate response regulator OmpR have been shown to regulate the expression of genes encoding the outer membrane porin proteins, OmpF and OmpC, in response to changes in the medium osmolarity [4]. The EnvZ/OmpR system is among the best characterized histidyl-aspartyl phosphotransfer systems, but the sensory mechanism of EnvZ is not well understood at present. Understanding how cells sense and respond to osmolarity changes in their environment requires molecular and structural characterization of osmo-responsive proteins.

EnvZ is a 450-residue inner membrane histidine kinase with typical domain architecture: an N-terminal cytoplasmic tail (residues 1–15), two transmembrane domains (TM1, residues 16–34, and TM2, residues 163–179) flanking a periplasmic domain ($EnvZ_{per}$, residues 35–162) and a cytoplasmic domain (residues 180–450) (Figure 1A) [5]. The cytoplasmic domain has been dissected further into a linker domain (residues 180–222), domain A (dimerization and histidine-containing domain, residues 223–289) and domain B (catalysis-assisting and ATP-binding domain, residues 290–450) [6]. Domain A and domain B are central to the autophosphorylation function of EnvZ, which mediates coupling between the environmental sensing and activation of OmpR by phosphorylation of an aspartate residue. The initial step of this signal transduction mechanism is the sensing of an environmental change that may involve unknown ligand binding to EnvZ. Usually, the ligand-binding domain of the receptor is located in the periplasm, where it interacts with a small molecule or the binding protein of a small molecule [7]. Specifically, EnvZ responds to an extracellular stimulus by ATP-dependent autophosphorylation of the conserved His^{243} residue located in the cytoplasmic region of the kinase. This is followed by a transfer of the phosphoryl group to the conserved Asp^{55} residue on OmpR, which in turn gives rise to a conformational change in the response regulator that alters its affinity to the *OmpC* and *OmpF* promoters that it regulates. The cytosolic domain of EnvZ functions as a dimer that harbours both a kinase and a phosphatase activity [8]. Once activated in response to a change in medium osmolarity, EnvZ undergoes a modulation of these activities, thereby regulating the cellular concentration of phosphorylated OmpR, which controls the reciprocal expression of OmpF and OmpC [9,10].

To gain insight into transmembrane signal transduction mechanisms of EnvZ, several groups have constructed aspartate- and ribose-responsive chimaeric proteins consisting of the N-terminal periplasmic and transmembrane domains of the Tar or Trg chemoreceptors respectively, and the cytoplasmic catalytic domain of EnvZ [11,12]. Studies on these chimaeric proteins [13,14], combined with mutagenesis analysis [15,16], have shown that the transmembrane, as well as the linker helices, plays a role in signal propagation. While *in vitro* studies on reconstituted *E. coli* EnvZ have shown a response to changes in K^+ concentration [17], the mechanisms underlying the sensing function have not been elucidated. Replacement of up to 91 amino acids (Met^{56}–Arg^{146}) from the C-terminal region of $EnvZ_{per}$ with the non-homologous periplasmic domain of PhoR had no effect on the regulation of OmpF and OmpC expression [18], thus putting in question the role of $EnvZ_{per}$ in sensing osmolarity signal(s). More recently, however, mutagenesis studies have suggested that leucine residues

Abbreviations used: AUC, analytical ultracentrifugation; CT domain, C-terminal core domain; $EnvZ_{per}$, periplasmic domain of EnvZ; HSQC, heteronuclear single quantum coherence; IPTG, isopropyl β-D-thiogalactoside; Omp, outer membrane porin; TM, transmembrane domain; UT, untagged.

[1] To whom correspondence should be addressed (email mikura@uhnres.utoronto.ca).

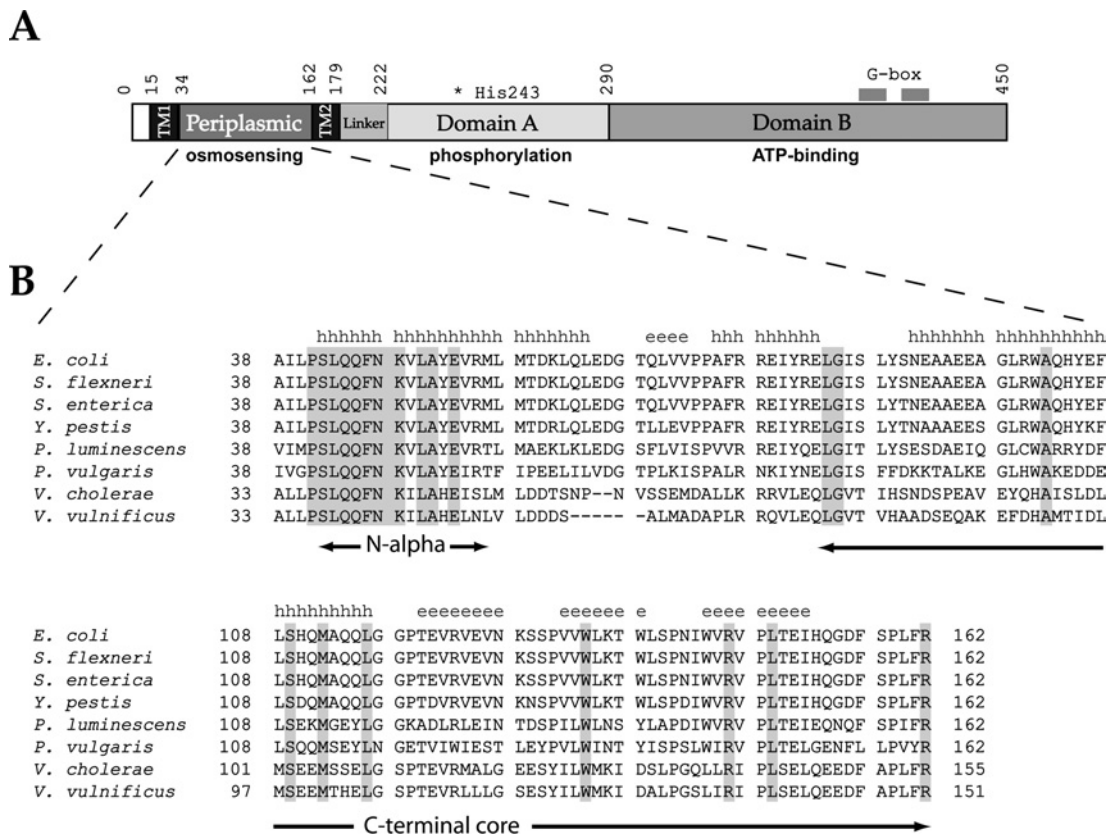

Figure 1 Structural characteristics of the EnvZ osmosensor

(**A**) Schematic representation of subdomain composition of *E. coli* histidine kinase EnvZ. The conserved active site His^{243} and G-boxes in the cytoplasmic domain and the function of each domain are highlighted. (**B**) Sequence alignment of $EnvZ_{per}$s from different γ-proteobacterial species (*Shigella flexneri*, *Salmonella enterica*, *Yersinia pestis*, *Pseudomonas luminescens*, *Proteus vulgaris*, *Vibrio cholerae* and *Vibrio vulnificus*). Residues that are conserved among the different species are highlighted, and the predicted secondary structure of the periplasmic domain is shown above the sequence (h indicates α-helical structure, and e indicates β-sheets). The predicted N-terminal α-helix (Ser^{42}–Leu^{57}) and the trypsin-resistant CT domain (Glu^{83}–Arg^{162}) are also indicated.

in a conserved N-terminal region of the periplasmic domain (Pro^{41}–Glu^{53}) may play a role in osmotic signal transduction by mediating dimerization of $EnvZ_{per}$ [19,20]. In the present study, we have characterized the structural properties of $EnvZ_{per}$ and provide evidence that it consists of two domains. In light of the structural characteristics of the periplasmic domains, we discuss possible molecular and structural mechanisms for environmental sensing and transmembrane signal transduction of EnvZ.

EXPERIMENTAL

Plasmid construction

pET15b (Novagen) was used to construct a His_6–$EnvZ_{per}$ (Ala^{38}–Arg^{162}) fusion protein. *E. coli* $EnvZ_{per}$ was generated by PCR from pDR200, an EnvZ plasmid. *Nde*I and *Bam*HI restriction endonuclease sites and a C-terminal stop codon were introduced using PCR primers (sense primer, 5′-CTG*CATATG*GCGATTTTGCCGAGCCTCCAGCA-3′; antisense primer, 5′-CGC*GGATCCTTA*GCGGAACAGCGGAGAGAAATCGC-3′; italicized bases indicate restriction sites and the stop codon). The PCR product was digested with *Nde*I and *Bam*HI and was subcloned into the corresponding sites in pET15b downstream from the His_6-tag and a thrombin-cleavage site and designated as pET15b-$EnvZ_{per}$. The L43A (Leu^{43} → Ala), L50A, L57A, L43/50A and L43/57A mutations were constructed using the QuikChange site-directed mutagenesis kit (Stratagene). All constructs were verified by sequencing to ensure that no mutations were introduced during PCR amplification.

Expression and purification

E. coli strain BL21(DE3) was used for expression of pET15b-$EnvZ_{per}$. Cells were grown to exponential phase in 2 litres of LB (Luria–Bertani) broth supplemented with 100 μg/ml ampicillin, followed by 3 h of IPTG (isopropyl β-D-thiogalactoside) induction (1 mM) at 37 °C. His_6–$EnvZ_{per}$ fusion protein was expressed into inclusion bodies. Cells were harvested and lysed by sonication in lysis buffer A [50 mM Tris/HCl, pH 8.2, 500 mM NaCl, 15 % (v/v) glycerol and 1 % (v/v) Nonidet P40]. The lysate was centrifuged at 11 000 ***g*** in an SS34 rotor (Sorval) for 20 min at 4 °C. The resulting pellet containing the His_6–$EnvZ_{per}$ fusion protein was then subjected to three freeze–thaw cycles to help break up the cell wall and release the expressed protein from the inclusion bodies. The pellet was treated further by sonication in lysis buffer B [6 M guanidinium chloride, 50 mM Tris/HCl, pH 8.2, 500 mM NaCl and 15 % (v/v) glycerol]. Insoluble cell debris was removed by centrifugation at 17 500 ***g*** in an SS34 rotor (Sorval) for 30 min at 4 °C. Soluble denatured His_6–$EnvZ_{per}$ fusion protein was purified over a Ni-NTA (Ni^{2+}-nitrilotriacetate) column (Qiagen) pre-equilibrated with lysis buffer B and eluted with 250 mM imidazole. Fractions containing the denatured protein were pooled and sequentially dialysed against buffer containing 5 M, then 4 M, and, finally, 3 M guanidinium chloride. The dialysed protein was concentrated to 20 mg/ml and refolded

by rapid dilution to 0.1 mg/ml into refolding buffer C [50 mM Mes, pH 6.5, 10.56 mM NaCl, 0.44 mM KCl, 0.055 % (v/v) poly-(ethylene glycol) 3350, 550 mM guanidinium chloride, 1.1 mM EDTA, 440 mM sucrose and 550 mM L-arginine]. The protein was then dialysed against buffer D (50 mM sodium acetate, pH 5, and 50 mM NaCl) and stored at 4 °C for further use.

Solubility screens

To improve the solubility of $EnvZ_{per}$ for NMR spectroscopy and biophysical analysis, $EnvZ_{per}$ was concentrated to its solubility limit (0.5 mg/ml in 20 mM sodium acetate, pH 5, and 50 mM NaCl). Solubility was then assessed in 24 different buffer and pH combinations at room temperature (20 °C) using a variation of the microdrop screen [21]. The buffers used were Mes, sodium acetate, sodium and potassium phosphate, Tris/HCl and Hepes. Each buffer was used at 50 mM concentration. The pH range of the screen was 4–9. After the initial screening for buffer and pH combinations, a second solubility screen was set up for varying concentrations of NaCl and KCl. Finally, a third screen was set up for additives that might help stabilize the protein and reduce protein aggregation. The additives tested were glycine, arginine, sodium perchlorate, CHAPS and Triton X-100.

Size-exclusion chromatography

Analytical gel-filtration analysis was carried out on a Superdex 75 HR 10/30 column using an AKTA Purifier system (Amersham Biosciences). Protein samples of 400 μl were loaded at a concentration of 0.5 mg/ml and eluted over 1.2 column volumes at a flow rate of 0.5 ml/min. The column was calibrated using the following molecular-mass standards: BSA (66.5 kDa), ovalbumin (43 kDa), chymotrypsinogen A (25 kDa), RNase A (14.8 kDa) and aprotinin (6.5 kDa).

AUC (analytical ultracentrifugation)

Sedimentation experiments were performed at 20 °C on a Beckman XLI Analytical Ultracentrifuge using an AN50-Ti rotor and sapphire windows. The sedimentation equilibrium experiments using six-channel charcoal-Epon cells were performed at 26000, 32000, 36000 and 40000 rev./min. Three different sample concentrations were used for each analysis: 0.3, 0.6 and 0.9 mg/ml. Samples were left for 14 h at each centrifugation speed to ensure that equilibrium was reached before absorbance measurements were taken. Global analysis of the data was performed using XL-A/XL-I data analysis software (version 4.0) from Beckman Instruments.

Pull-down assay

All assays were performed using 15 μl of TALON metal-affinity resin beads (Clontech) in 200 μl PCR tubes in 20 mM Tris/HCl, pH 7, 10 mM CHAPS, 200 mM NaCl and 5 mM imidazole. His_6-tagged protein (4.5 μg) was used as bait and 16 μg of untagged (UT) protein was used as prey in a 50 μl assay volume. The assay mixture was incubated for 30 min at room temperature with shaking. Unbound protein was removed by washing the beads three times with 100 μl of Tris/HCl, pH 7, 5 mM CHAPS, 200 mM NaCl and 5 mM imidazole. Protein complexes were analysed by adding 20 μl of 2× sample buffer supplemented with 200 mM imidazole, boiling for 10 min and separating by SDS/PAGE. Densitometry analysis was used to quantify the amount of protein that was pulled-down. To normalize for beads lost during washing, the data were reported as the ratio of UT to His_6-tagged protein.

CD

CD spectra were acquired on an AVIV spectrometer model 62DS using a 0.1 cm cell at 25 °C. Spectra were collected over a wavelength range of 200–260 nm or 250–300 nm at 0.5 nm resolution, a bandwidth of 1.0 nm and an averaging time of 20 s. Final spectra were the sum of five scans. For thermal denaturation experiments, the CD spectrum of 0.4 mg/ml $EnvZ_{per}$ in 20 mM sodium acetate, pH 5, 50 mM NaCl and 10 mM CHAPS was recorded at 1 °C increments from 25 to 95 °C, and the molar ellipticity at 216 and 222 nm was monitored.

NMR spectroscopy

All NMR data were collected at 27 °C (probe temperature) on a Varian Unity Inova 600 MHz spectrometer equipped with a 5 mm triple resonance probe with XYZ gradients and operating proton frequency of 600.256 MHz. ^{15}N-^{1}H HSQC (heteronuclear single quantum coherence) experiments were recorded with 576 and 256 complex points in t_2 and t_1 respectively. Final data sets comprised 1024 and 2048 real points with digital resolution of 1.8 and 4.4 Hz/point in F_1 and F_2 respectively. All data were processed and analysed with NMRPipe and NMRDraw.

RESULTS AND DISCUSSION

Purification of recombinant $EnvZ_{per}$ domain

E. coli $EnvZ_{per}$ (Lys^{48}–Arg^{162}) was purified previously as an MBP (maltose-binding protein)-fused recombinant protein [22]. The protein expression and yield reported were too low for detailed biophysical analysis, and the construct used lacked seven highly conserved N-terminal amino acids from the periplasmic region (Pro^{41}–Asn^{47}) (Figure 1B). In the present study, we fused nearly the entire *E. coli* $EnvZ_{per}$ (Ala^{38}–Arg^{162}) to an N-terminal His_6-tag in order to facilitate protein purification by Ni^{2+}-affinity chromatography. The resulting fusion protein His_6–$EnvZ_{per}$ was overexpressed in *E. coli* BL21(DE3) strain. After induction with 1 mM IPTG, His_6–$EnvZ_{per}$ comprised more than 30 % of total cellular protein (see Supplemental Figure S1 at http://www.BiochemJ.org/bj/385/bj3850255add.htm). However, more than 90 % of the His_6–$EnvZ_{per}$ fusion protein was insoluble. The insoluble protein was solubilized with 6 M guanidinium chloride and Ni^{2+}-affinity chromatography was performed under these denaturing conditions. The denatured protein was refolded by stepwise dilution of guanidinium chloride concentration to 3 M via dialysis, followed by rapid dilution into refolding buffer. Some precipitation was observed after refolding, and was removed by centrifugation and filtering through a 0.22-μm-pore-size filter. An estimated 40 % of the protein was recovered after refolding. The protein was then dialysed against 20 mM Tris/HCl, pH 8, 150 mM NaCl and digested with thrombin to remove the His_6-tag. The final protein contains Gly-Ser-His-Met from the pET15b vector at the N-terminus, followed by $EnvZ_{per}$ (amino acids 38–162). The identity of the protein was confirmed by MS and the molecular mass of the protein was measured to be 14906 Da, which is in agreement with the expected molecular mass of 14864 Da.

The protein concentration after purification was only 50 μg/ml. Attempts to concentrate the protein for biophysical analyses resulted in the protein precipitating out of solution. Thus solubility screens were set up using an adaptation of the microdrop screen [21], as described in the Experimental section. In an initial screen testing pH and buffer conditions, considerable precipitation was observed, particularly at conditions higher than pH 7 in Tris/HCl and Hepes buffers. We found that the protein became more

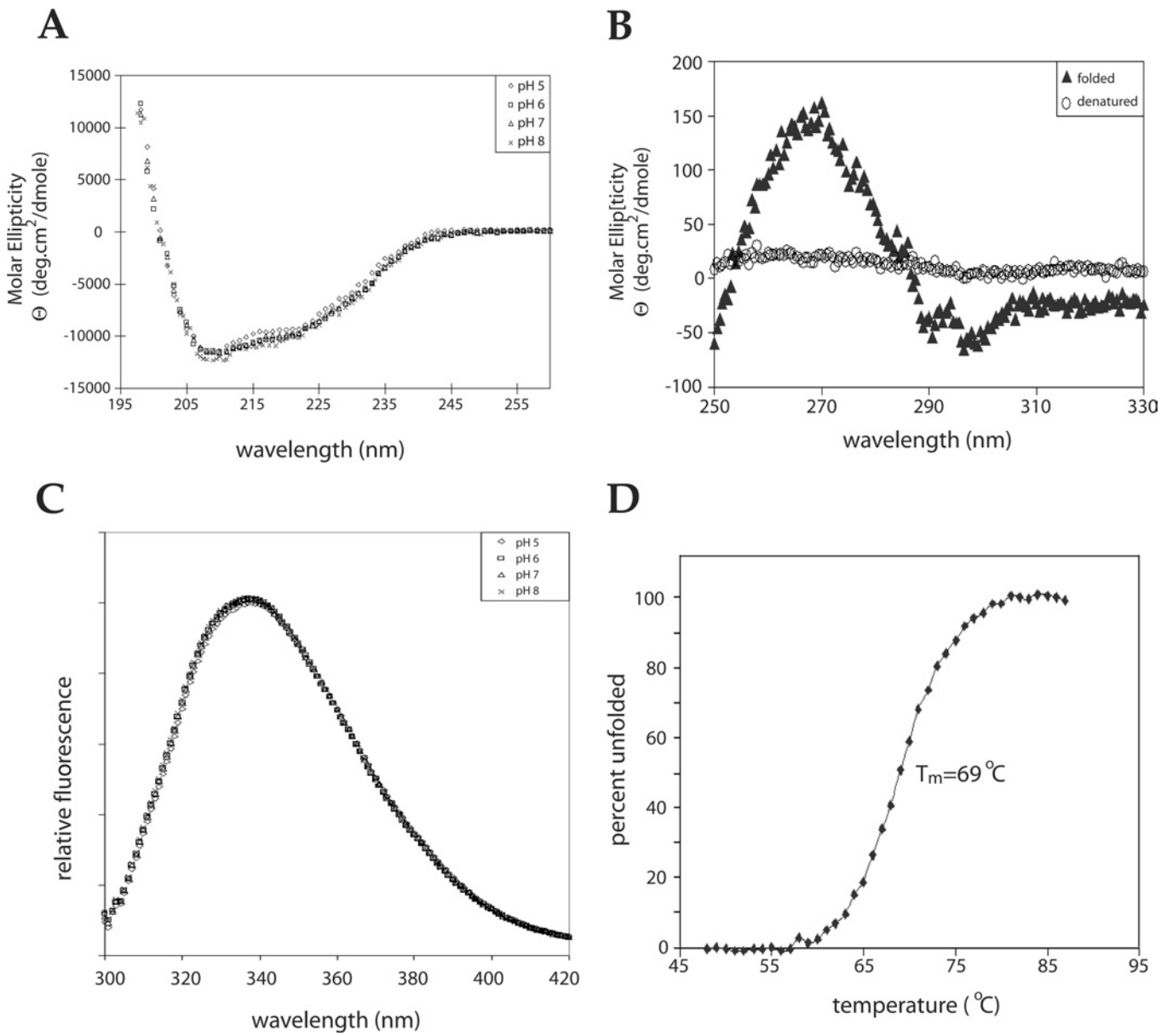

Figure 2 Biophysical characterization of $EnvZ_{per}$

(**A**) Far-UV CD analysis of 100 μM refolded $EnvZ_{per}$ in 5 mM sodium acetate, pH 5, and 50 mM NaCl; 5 mM potassium phosphate, pH 6, and 50 mM NaCl; 5 mM potassium phosphate, pH 7, and 50 mM NaCl; and 5 mM potassium phosphate, pH 8, and 50 mM NaCl. (**B**) Near-UV CD analysis of 300 μM native (5 mM sodium acetate, pH 5, and 50 mM NaCl) and denatured (3 M guanidinium chloride and 50 mM NaCl) $EnvZ_{per}$. (**C**) Intrinsic tryptophan fluorescence analysis of 50 μM $EnvZ_{per}$ at pH 5–8. (**D**) Thermal stability of $EnvZ_{per}$ as measured by a change in molar ellipticity at 222 nm. T_m, melting point.

soluble in sodium acetate buffer at pH 5. In a second screen to refine further the conditions by varying salt concentration from 50 to 500 mM NaCl, we observed that protein solubility was enhanced at lower salt concentrations. Thus $EnvZ_{per}$ protein was dialysed against 20 mM sodium acetate, pH 5, and 50 mM NaCl, and then concentrated to 0.5 mg/ml.

Structural characterization

The domain arrangement of *E. coli* EnvZ is depicted in Figure 1(A). The sequence of $EnvZ_{per}$ from *E. coli* was aligned against the corresponding sequences from other γ-proteobacteria (Figure 1B). PHD (Profile network from HeiDelberg) secondary structure prediction [23] (Figure 1B) estimates this region of EnvZ to consist of 45 % α-helices and 22 % β-sheets. ClustalW multiple sequence alignment revealed a low (16 %) overall sequence identity in $EnvZ_{per}$ between the different γ-proteobacterial species. However, a predicted N-terminal helix (hereafter named N-alpha, residues Ser^{42}–Leu^{57}) is highly conserved (69 % sequence identity) among these species.

To ascertain that purified $EnvZ_{per}$ was properly folded, we performed several biophysical analyses including far and near UV CD, as well as intrinsic fluorescence spectroscopy. The far UV CD spectra of $EnvZ_{per}$ at pH 5–8 were identical, exhibiting strong peaks of negative ellipticity at 208 nm and 222 nm (Figure 2A). Analysis of the CD spectra using the K2D software

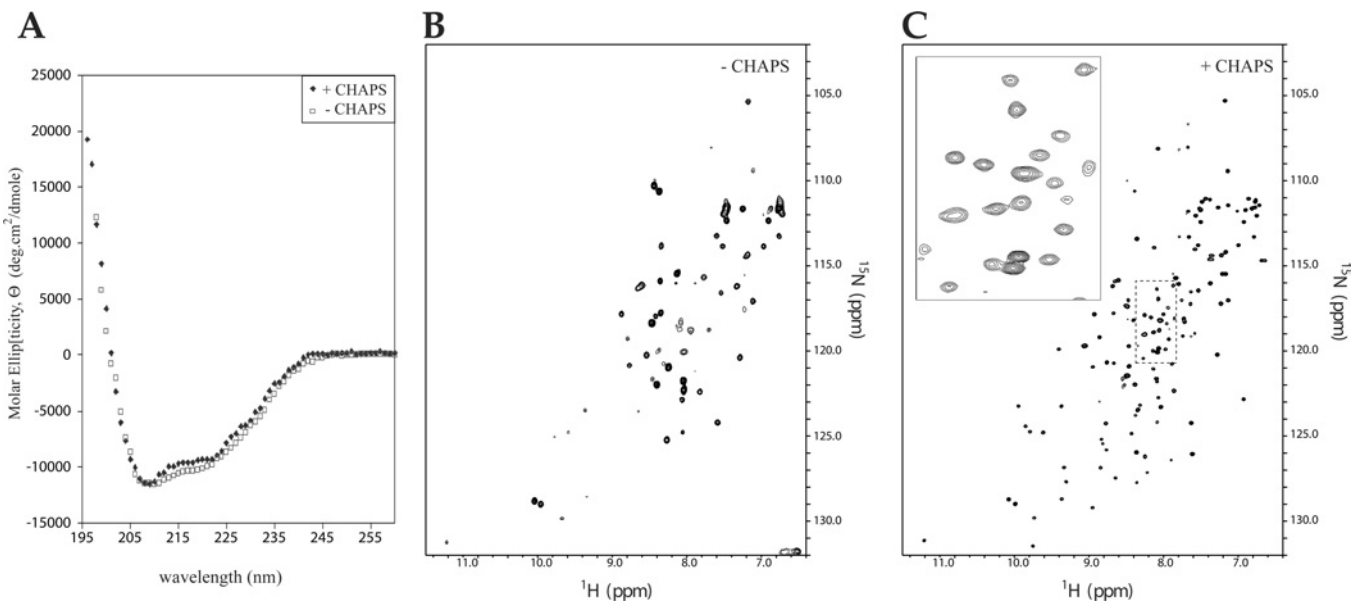

Figure 3 Structural analysis of $EnvZ_{per}$ in the presence and absence of CHAPS

(**A**) Far UV CD analysis of 100 μM $EnvZ_{per}$ in the presence (◆) and absence (□) of 1 mM CHAPS in 5 mM sodium acetate, pH 5, and 50 mM NaCl buffer. (**B**) ^{15}N-edited HSQC spectra of 0.3 mM $EnvZ_{per}$ in 20 mM sodium acetate, pH 5, and 50 mM NaCl, and (**C**) 0.9 mM $EnvZ_{per}$ in 20 mM sodium acetate, pH 5, 50 mM NaCl, and 10 mM CHAPS.

indicates that $EnvZ_{per}$ consists of 41 % α-helical and 20 % β-sheet structures. This is in close agreement with data reported previously [22], as well as the PHD prediction of 45 % α-helices and 22 % β-sheets in the corresponding sequence of EnvZ. To determine that $EnvZ_{per}$ is properly folded into tertiary structure, we measured the near UV (250–330 nm) CD spectrum, which is indicative of the chemical environment of aromatic residues, such as phenylalanine (250–270 nm), tyrosine (270–290 nm) and tryptophan (280–300 nm). $EnvZ_{per}$, denatured in the presence of 3 M guanidinium chloride, displayed no apparent signal in this near UV region, while refolded $EnvZ_{per}$ showed significant near-UV signals, thus indicating that $EnvZ_{per}$ is folded into a well-defined structure (Figure 2B).

$EnvZ_{per}$ has four tryptophan residues (residues 101, 134, 138 and 144) in its sequence. Intrinsic tryptophan fluorescence is a sensitive probe of local and global conformation in proteins [24], and has commonly been used to investigate protein conformational stability upon addition of chemical denaturants, such as urea and guanidinium chloride [25–27]. We measured the intrinsic tryptophan fluorescence of $EnvZ_{per}$ to probe mainly for pH-sensitivity of these tryptophan residues in the refolded protein. In the pH range 5–8, no major change in the intrinsic fluorescence was observed (Figure 2C). We then examined temperature melting using CD spectroscopy at 222 nm (Figure 2D). The results indicate that $EnvZ_{per}$ undergoes a thermal transition between 65 and 75 °C, with 50 % of the protein denaturing at 69 °C. This thermal denaturation of $EnvZ_{per}$ was irreversible. These data indicate that $EnvZ_{per}$ is relatively stable at the neutral pH range 5–8, and at temperatures below 65 °C.

^{1}H-^{15}N HSQC spectra of $EnvZ_{per}$ under the conditions tested thus far showed a few well-resolved sharp cross-peaks and a cluster of broad peaks (Figure 3B). This NMR spectrum strongly suggests severe exchange broadening, which may be caused by protein oligomerization. We therefore performed an extensive solubility screen with various additives that might enhance protein solubility, including glycine, arginine, sodium perchlorate, CHAPS and Triton X-100 [28]. Among the additives tested, Triton X-100 and sodium perchlorate showed no change in solubility, while glycine, arginine and CHAPS resulted in improved solubility. We chose CHAPS for NMR studies, as it yielded the highest solubility without affecting the secondary structure as measured by CD spectroscopy (Figure 3A). $EnvZ_{per}$ was concentrated to 0.9 mM in the presence of 10 mM CHAPS and ^{1}H-^{15}N HSQC spectra were recorded at 27 °C (Figure 3C). In the presence of CHAPS, the HSQC spectrum improved dramatically, displaying 134 well-resolved peaks, including 26 distinct peaks from side chain NH_2 groups of asparagine and glutamine. This leaves 108 peaks from backbone NH_2 groups. The expected number of backbone peaks is 120 (129 amino acid residues in $EnvZ_{per}$, excluding the N-terminal glycine residue and the eight proline residues which have no backbone amide proton). Clearly, the addition of CHAPS helps prevent protein oligomerization, presumably by reducing non-specific hydrophobic interactions between $EnvZ_{per}$ molecules.

Domain mapping

To assess whether $EnvZ_{per}$ is made of a single globular domain or multiple subdomains, we employed the standard limited proteolysis approach [29]. Limited tryptic digestion of $EnvZ_{per}$ (molecular mass 14.8 kDa) resulted in a proteolytically resistant polypeptide with an apparent molecular mass of 10 kDa (Figure 4A). Polyacrylamide gel extraction of this fraction followed by MS/MS sequencing showed two species (differing by four amino acids) corresponding to the C-terminus of $EnvZ_{per}$. The predominant species corresponded to residues Glu^{83}–Arg^{162} of $EnvZ_{per}$, and the minor species contained the additional residues Glu^{79}–Arg^{82} at the N-terminus. CD analysis of the major trypsin-resistant fragment confirmed that it is well-folded, with a mixed α-helical and β-sheet character (Figure 4B). K2D analysis of this CD spectrum indicated that this fragment consists of 31 % α-helix and 30 % β-sheet, as compared with the 41 % α-helical and

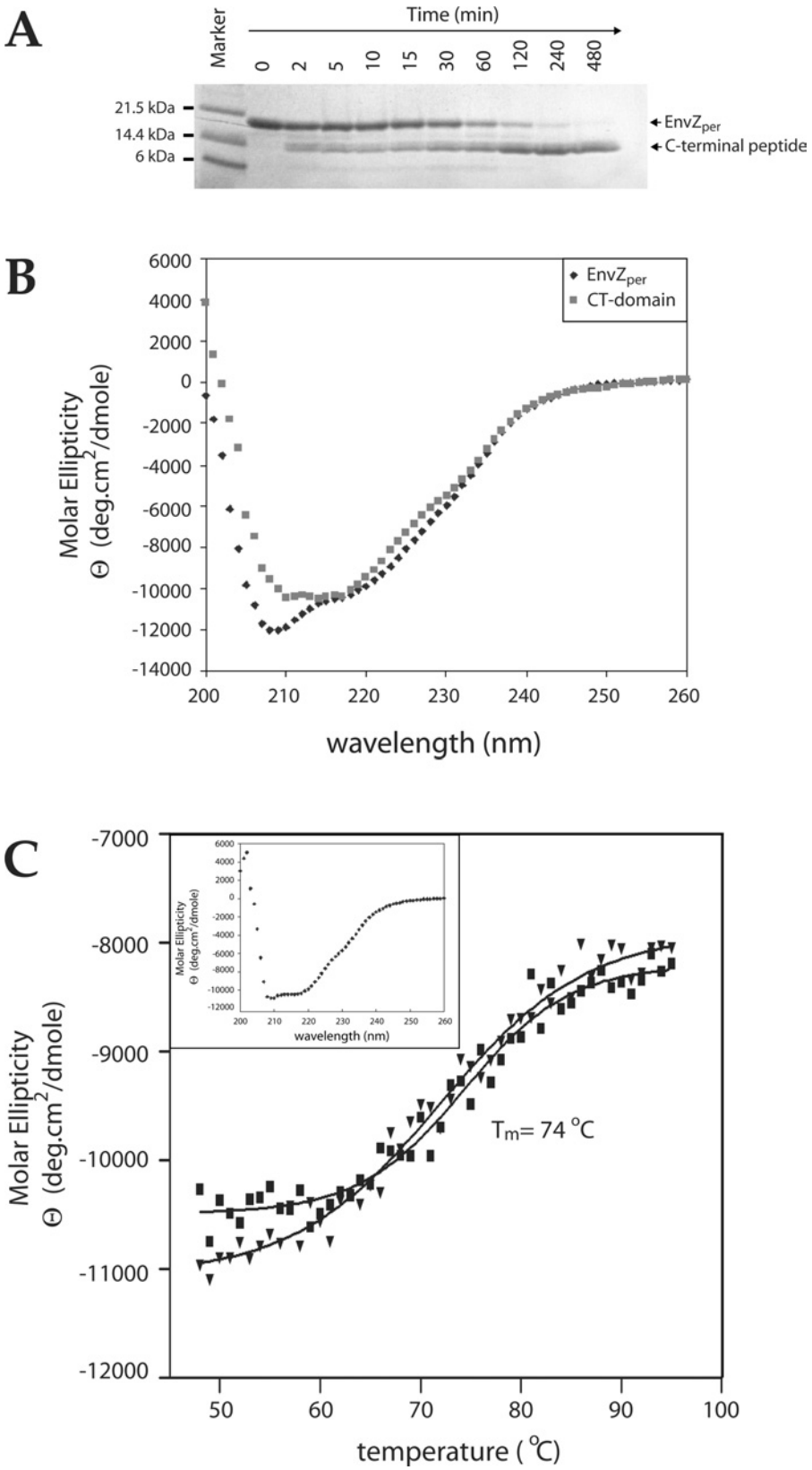

Figure 4 Domain mapping of $EnvZ_{per}$

(**A**) SDS/PAGE analysis of limited tryptic proteolysis of $EnvZ_{per}$. $EnvZ_{per}$ was incubated with trypsin at a 20:1 molar ratio at 4 °C in 20 mM potassium phosphate, pH 8, and 50 mM NaCl, and aliquots were collected at 0, 2, 5,10, 15, 30, 60, 120, 240 and 480 min. (**B**) Far-UV CD analysis of 100 μM CT domain (■) and 100 μM $EnvZ_{per}$ (◆) in 5 mM potassium Tris, pH 8, and 50 mM KCl. (**C**) Thermal stability of $EnvZ_{per}$ CT domain as measured by a change in molar ellipticity at 215 nm. The denaturation curve is denoted by (■), while the renaturation curve by (▼). The insert is a CD spectrum of the protein sample after thermal denaturation and renaturation. T_m, melting temperature.

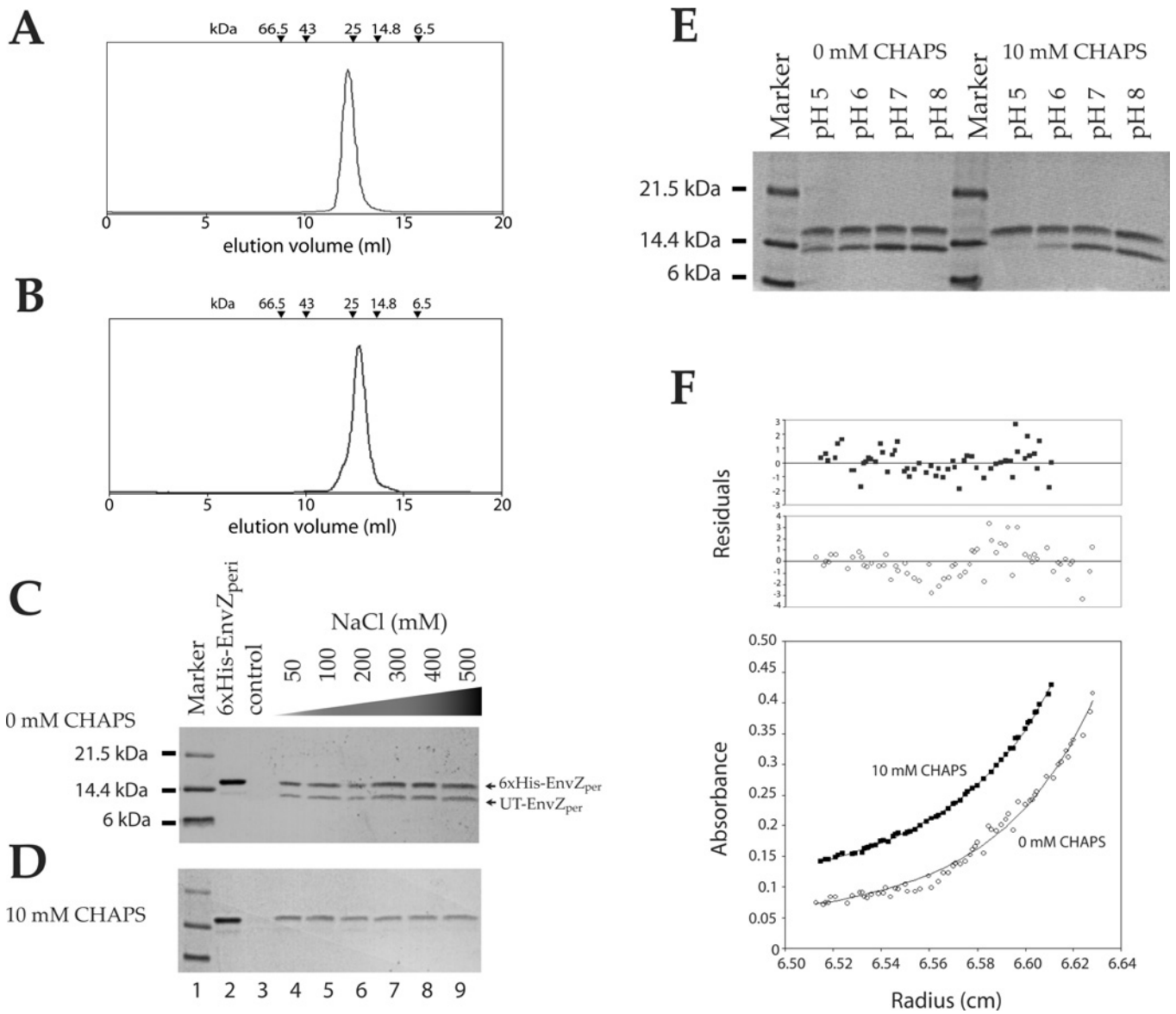

Figure 5 Dimerization of $EnvZ_{per}$ in solution

(**A** and **B**) Chromatogram of size-exclusion analysis of 100 μM full-length $EnvZ_{per}$ and CT domain on a Superdex 75 column respectively. The elution volume of protein standards is indicated on top of the chromatogram. (**C** and **D**) SDS/12 % PAGE analysis of pull-down assays of His_6-tagged $EnvZ_{per}$ and UT-$EnvZ_{per}$ at pH 5. The assays in (**C**) and (**D**) were performed at pH 5 at various NaCl concentrations. The assays were performed on the following samples: lane 2, His_6–$EnvZ_{per}$; lane 3, UT-$EnvZ_{per}$; lanes 4–9, His_6–$EnvZ_{per}$ and UT-$EnvZ_{per}$ at the indicated NaCl concentrations. (**E**) SDS/PAGE analysis of pull-down assay of $EnvZ_{per}$ in the presence and absence of CHAPS at various pHs. (**F**) Representative sedimentation equilibrium data obtained for 50 μM $EnvZ_{per}$ at pH 8 in the presence and absence of 10 mM CHAPS. Only the data at 40 000 rev./min is represented.

20 % β-sheet content of the full-length periplasmic domain. Subtraction of the secondary-structure content of the C-terminal fragment (hereafter named CT domain) from that of the full-length periplasmic region suggests that the N-terminal region of $EnvZ_{per}$ (residues Ala^{38}–Arg^{78}) consists of 57 % α-helices and 6 % β-sheets. The thermal denaturation profile of the CT domain indicated a melting temperature of 74 °C (Figure 4C), which is 5 °C higher than that of the full-length $EnvZ_{per}$. The CT domain is remarkably stable and resistant to tryptic proteolysis and, unlike $EnvZ_{per}$, can unfold and re-fold reversibly upon heating and cooling. These data provide compelling evidence that $EnvZ_{per}$ consists of a 10 kDa CT core domain of an α/β-fold, with an additional α-helical segment (N-alpha) at the N-terminus.

$EnvZ_{per}$ oligomerizes via the CT domain

Although the cytoplasmic domain of *E. coli* EnvZ can form a homodimer, mainly via the four-helix-bundle domain containing the active site His^{243} [30], the nature of the oligomeric state of the periplasmic region remains structurally uncharacterized. Evidence from disulphide cross-linking of cysteine residues inserted into the N-alpha domain of the periplasmic region suggested that it can engage in a dimeric association *in vivo* [20]. However, it is uncertain whether the N-alpha domain solely mediates dimerization. The chromatogram from Superdex-75 size-exclusion chromatography of $EnvZ_{per}$ showed a well-folded single species with a molecular mass of 28 kDa (Figure 5A). This

indicates that $EnvZ_{per}$ alone can form a dimer in solution. The same size-exclusion chromatographic analysis of the CT domain showed that this polypeptide is also a dimer with an apparent molecular mass of 20 kDa in solution (Figure 5B). These results demonstrate that $EnvZ_{per}$ dimerization is predominantly mediated by the CT domain and does not require the N-alpha domain for homodimeric association.

Further validation of the dimeric nature of $EnvZ_{per}$ in the presence and absence of CHAPS was obtained from AUC, as well as pull-down assays. The pull-down assay was performed at varying NaCl concentrations at pH 5 in the absence (Figure 5C) and presence (Figure 5D) of 10 mM CHAPS. The assays were performed using the Co^{2+}-based affinity resin due to reduced non-specific binding relative to that of the Ni^{2+}-based affinity resin (Figures 5C and 5D, lanes 3). The ability of His_6–$EnvZ_{per}$ to pull-down UT-$EnvZ_{per}$ was used to assay for protein oligomerization. In the absence of CHAPS, UT-$EnvZ_{per}$ was detected in the pull-down assay at all salt concentrations tested (Figure 5C, lanes 4–9). This demonstrates that the oligomerization of $EnvZ_{per}$ occurs in the absence of CHAPS in solution, and the lack of sensitivity of this observed oligomerization to salt concentration (up to 0.5 M NaCl) suggests that the $EnvZ_{per}$ oligomerization is mediated by hydrophobic interactions. Protein oligomerization is significantly reduced upon the addition of 10 mM CHAPS (Figure 5D, lanes 4–9). Furthermore, this oligomerization increases when the pH is increased from 5 to 8 both in the presence and absence of 10 mM CHAPS (Figure 5E). Although little or no UT-$EnvZ_{per}$ was observed in the pull-down assay at pH 5 in the presence of CHAPS, AUC analysis of $EnvZ_{per}$ (performed at concentrations higher than those used for the pull-down assays) revealed that $EnvZ_{per}$ remains largely dimeric at pH 5. Quantitative analysis of the AUC data showed that at pH 5 in the presence of 10 mM CHAPS, $EnvZ_{per}$ exists in a monomer–dimer equilibrium with an association constant (K_a) of 0.58×10^4 M^{-1}. At pH 8, this K_a value was raised slightly to 1.8×10^4 M^{-1} (Figure 5F). In the absence of CHAPS, the AUC data could not fit well with a single two-state model (Figure 5F), suggesting the presence of higher order oligomeric states. This is consistent with the observation that at high pH ($\geqslant 7$), and in the absence of CHAPS, $EnvZ_{per}$ undergoes non-specific aggregation resulting in severely broadened NMR spectra. These AUC data in combination with pull-down and NMR data indicate that at basic pH and in the absence of CHAPS, $EnvZ_{per}$ aggregates, at a slightly acidic pH and in the presence of CHAPS, $EnvZ_{per}$ is predominantly dimeric, and that CHAPS helps prevent high-order oligomerization.

Possible role for N-alpha domain in osmosensing

Yaku and Mizuno [20] have shown that cysteine substitution mutation of Leu^{43} and Leu^{50} in $EnvZ_{per}$ results in an increase in the kinase/phosphatase activity ratio of EnvZ, a phenotype that is observed under high-osmolarity conditions. A similar phenotype was observed for alanine substitution mutations at Leu^{43} [19] and Leu^{50} [20]. A role for conserved leucine residues (Leu^{43}, Leu^{50} and Leu^{57}) located in a predicted N-terminal amphoteric helix (Figure 6A) has been implicated in the propagation of osmotic signal by mediating dimerization of $EnvZ_{per}$ via hydrophobic interactions [19,20]. We performed alanine substitution mutagenesis on $EnvZ_{per}$ at these conserved leucine residues. Five different proteins were expressed and purified: L43A, L50A and L57A harbouring a single–alanine-substitution mutation, and L43/50A and L43/57A harbouring two. The effect of these mutations on $EnvZ_{per}$ dimerization was studied using the aforementioned pull-down assay. While all previously reported mutations at these leucine residues resulted in abrogation of EnvZ function [20], our

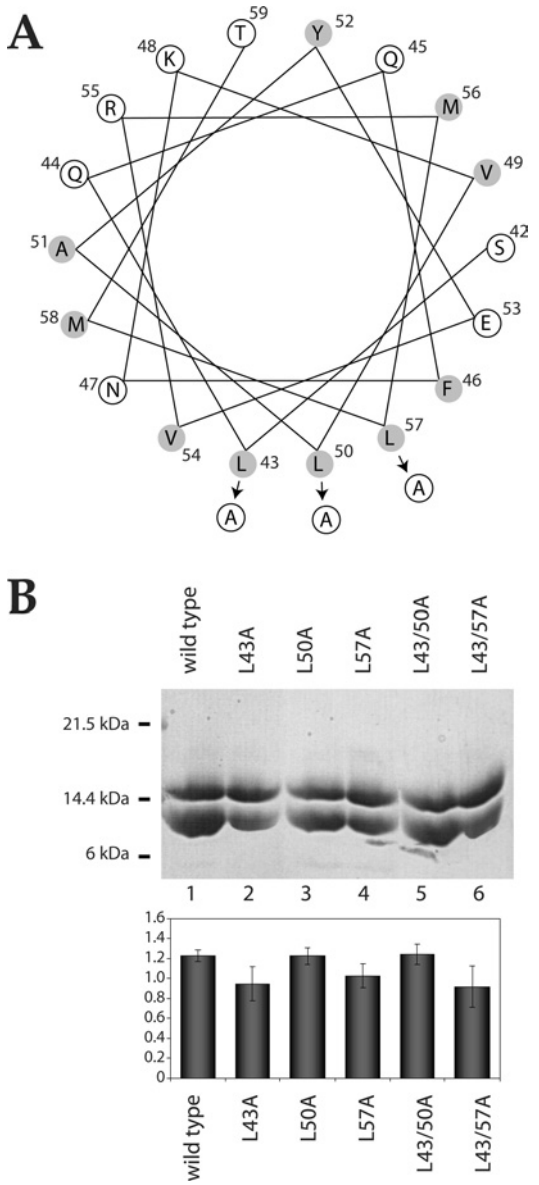

Figure 6 Role of conserved leucine residues in N-alpha in $EnvZ_{per}$ oligomerization

(**A**) Helical wheel representation of the predicted N-terminal α-helix of $EnvZ_{per}$. Hydrophobic residues are shaded. Arrows indicate the position of alanine substitution mutations. (**B**) SDS/PAGE analysis of pull-down assays of mutant $EnvZ_{per}$. Assays were performed in 20 mM potassium phosphate, pH 8, and 50 mM NaCl. Quantification of the ratio of UT/His_6-tagged protein by densitometry is represented by the histogram. Results are means $\pm$ S.D.

pull-down assays indicate that the alanine substitution mutations tested here have little effect on $EnvZ_{per}$ dimerization. Substitution of alanine for Leu^{43} and Leu^{50} resulted in a slight reduction in protein oligomerization (Figure 6B, lanes 2, 3 and 4), while substitution of Leu^{57} had no effect on protein oligomerization (Figure 6B, lanes 5 and 6). Moreover, there was no apparent change in either the structure or the oligomeric state of isolated wild-type or mutant $EnvZ_{per}$ upon addition of up to 400 mM KCl, 400 mM NaCl or 20 % sucrose (conditions that mimic high osmolarity), as measured by near-UV (250–330 nm) CD, intrinsic tryptophan fluorescence or the pull-down analysis. These results suggest that N-alpha is not required for the dimer formation of $EnvZ_{per}$, but is probably involved in fine-tuning of an active

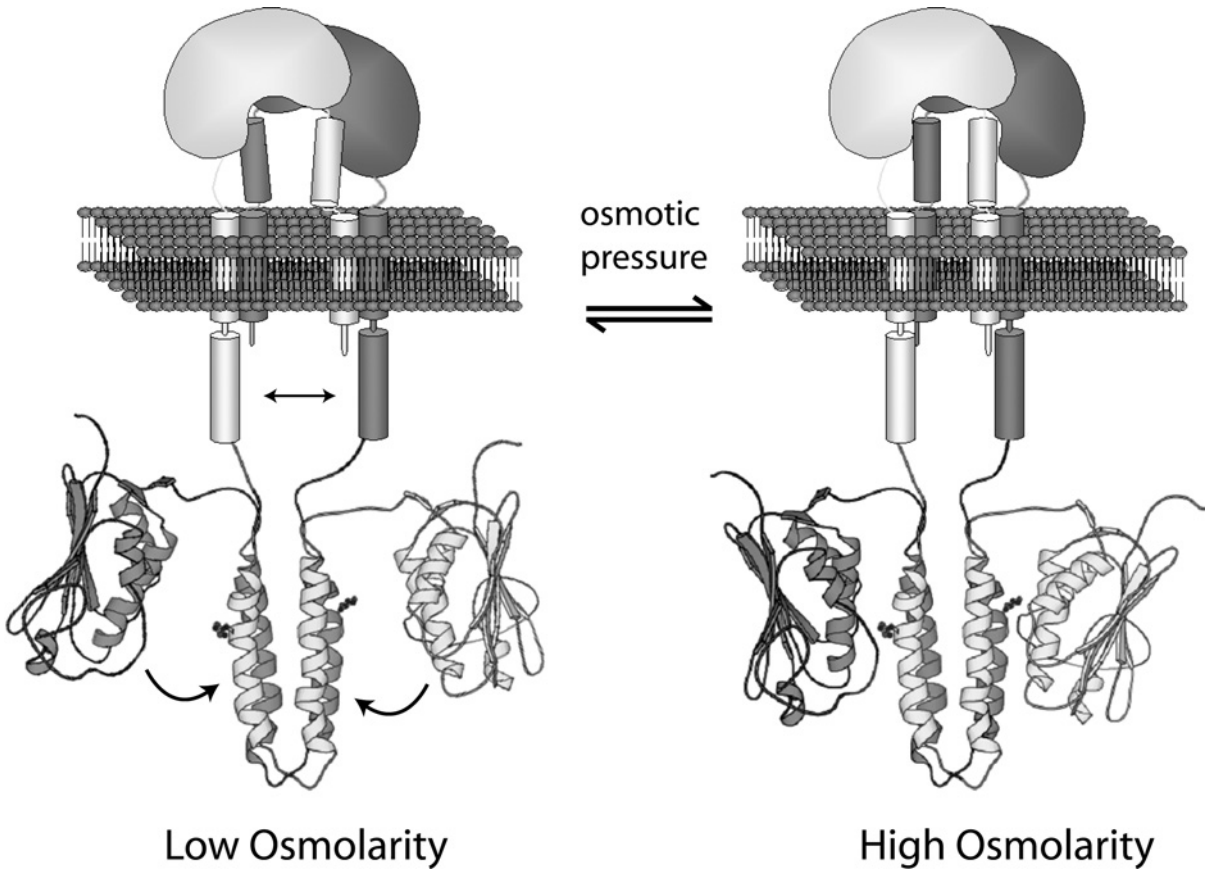

Figure 7 Model of osmosensing mediated by N-alpha in $EnvZ_{per}$

The CT domain maintains the dimeric structure of $EnvZ_{per}$, while the N-alpha dimer interface formed by the putative hydrophobic interaction acts as the signal transducer. In this model, high-osmolarity signals bring the two N-alpha domains close together, and low-osmolarity signals increase the distance between them, resulting in a fine-tuning of the overall structure of the periplasmic domain, which in turn leads to signal propagation across the membrane via sliding, rotating or tilting of the transmembrane helices. As a result, the topological relationship between domains A and B is changed, thus adjusting the kinase/phosphatase activity ratio of EnvZ.

conformation of the periplasmic region, possibly by hydrophobic interactions in the amphoteric helical motif [20]. Interestingly, the solution structure of the C-terminal region of the osmosensor ProP revealed a coiled-coil domain [31], which is thought to be important for osmotic activation of ProP [32].

Concluding remarks

$EnvZ_{per}$ has been thought to play a role in sensing an environmental stress in *E. coli*. As described above, previous studies [19,20] have pinpointed the importance of three conserved leucine residues in $EnvZ_{per}$, mutations of which have been shown to alter the kinase/phosphatase activity of the cytoplasmic domain, and ultimately, the expression of porin genes. These leucine residues reside at the N-terminal amphoteric helical region corresponding to the N-alpha domain identified in the present study. In addition, earlier deletion analysis has shown that removal of residues Met^{56}–Glu^{80} or Ile^{81}–Arg^{146}, and substitution of Met^{56}–Arg^{146} from $EnvZ_{per}$ with the non-homologous periplasmic domain of PhoR, had no effect on EnvZ function [18]. Our biophysical data indicate that $EnvZ_{per}$ contains a proteolytically resistant CT domain, corresponding to residues Glu^{83}–Arg^{162}, connected to the highly conserved N-alpha region. Taken together, the experimental evidence available thus far suggests that, while the CT domain is responsible for the stable dimer formation of $EnvZ_{per}$, the N-alpha segment may provide an additional 'arm' structure that is critical for transmitting the osmolarity change signal to the cytoplasmic domain of EnvZ (Figure 7). A mobility of N-alpha relative to the CT domain or the membrane interface may induce a slight change in domain orientation within the dimeric periplasmic region (Figure 7). Such possible fine-tuning of the N-alpha/N-alpha interaction may trigger further conformational change across the membrane, as suggested previously in models involving a piston-like differential sliding [33,34] or rotation [35,36] of TM2 relative to TM1. Finally, the environmental change probably involves yet to be identified ligands, both a small molecule and/or the binding protein of a small molecule, which may directly interact with the periplasmic region and/or some other part of the receptor. Further studies are needed to elucidate the exact mechanism by which EnvZ mediates environmental sensing and transmembrane signal transduction takes place in EnvZ.

We thank Sandy Go, Sylvia Ho and Dr Avijit Chakrabartty for their assistance with AUC analysis, Dr Yi-Min She for his assistance with MS analysis and sequencing, Dr Tapas K. Mal for his assistance with NMR data collection, and Dr Walid A. Houry for his assistance with the CD analysis. We also thank Jane Gooding, Takeshi Yoshida and Dr Ikuko Hayashi for critical reading of this manuscript. This work was supported by a grant from the Canadian Institutes of Health Research (CIHR) (to Mi.I.) and by Grant GM 19043 from the National Institutes of Health (to Ma.I.). Mi.I. held a CIHR Senior Investigator Award in 2003/2004 and is currently Canada Research Chair in Cancer Structural Biology. A.K. is supported by a grant from the American Foundation for AIDS Research.

REFERENCES

1 Mizuno, T. (1998) His-Asp phosphotransfer signal transduction. J. Biochem. (Tokyo) **123**, 555–563
2 Falke, J. J., Bass, R. B., Butler, S. L., Chervitz, S. A. and Danielson, M. A. (1997) The two-component signaling pathway of bacterial chemotaxis: a molecular view of signal transduction by receptors, kinases, and adaptation enzymes. Annu. Rev. Cell Dev. Biol. **13**, 457–512
3 West, A. H. and Stock, A. M. (2001) Histidine kinases and response regulator proteins in two-component signaling systems. Trends Biochem. Sci. **26**, 369–376
4 Mizuno, T., Wurtzel, E. T. and Inouye, M. (1982) Osmoregulation of gene expression. II. DNA sequence of the envZ gene of the ompB operon of *Escherichia coli* and characterization of its gene product. J. Biol. Chem. **257**, 13692–13698
5 Forst, S., Comeau, D., Norioka, S. and Inouye, M. (1987) Localization and membrane topology of EnvZ, a protein involved in osmoregulation of OmpF and OmpC in *Escherichia coli*. J. Biol. Chem. **262**, 16433–16438
6 Park, H., Saha, S. K. and Inouye, M. (1998) Two-domain reconstitution of a functional protein histidine kinase. Proc. Natl. Acad. Sci. U.S.A. **95**, 6728–6732
7 Muller-Dieckmann, H. J. and Kim, S.-H. (2003) Structure–function relationships: chemotaxis and ethylene receptors. In Histidine Kinases in Signal Transduction (Inouye, M. and Dutta, R., eds.), pp. 123–141, Academic Press, San Diego
8 Yang, Y. and Inouye, M. (1993) Requirement of both kinase and phosphatase activities of an *Escherichia coli* receptor (Taz1) for ligand-dependent signal transduction. J. Mol. Biol. **231**, 335–342
9 Jin, T. and Inouye, M. (1993) Ligand binding to the receptor domain regulates the ratio of kinase to phosphatase activities of the signaling domain of the hybrid *Escherichia coli* transmembrane receptor, Taz1. J. Mol. Biol. **232**, 484–492
10 Mizuno, T. and Mizushima, S. (1990) Signal transduction and gene regulation through the phosphorylation of two regulatory components: the molecular basis for the osmotic regulation of the porin genes. Mol. Microbiol. **4**, 1077–1082
11 Utsumi, R., Brissette, R. E., Rampersaud, A., Forst, S. A., Oosawa, K. and Inouye, M. (1989) Activation of bacterial porin gene expression by a chimeric signal transducer in response to aspartate. Science **245**, 1246–1249
12 Baumgartner, J. W., Kim, C., Brissette, R. E., Inouye, M., Park, C. and Hazelbauer, G. L. (1994) Transmembrane signalling by a hybrid protein: communication from the domain of chemoreceptor Trg that recognizes sugar-binding proteins to the kinase/phosphatase domain of osmosensor EnvZ. J. Bacteriol. **176**, 1157–1163
13 Jin, T. and Inouye, M. (1994) Transmembrane signaling: mutational analysis of the cytoplasmic linker region of Taz1-1, a Tar-EnvZ chimeric receptor in *Escherichia coli*. J. Mol. Biol. **244**, 477–481
14 Zhu, Y. and Inouye, M. (2003) Analysis of the role of the EnvZ linker region in signal transduction using a chimeric Tar/EnvZ receptor protein, Tez1. J. Biol. Chem. **278**, 22812–22819
15 Tokishita, S., Kojima, A. and Mizuno, T. (1992) Transmembrane signal transduction and osmoregulation in *Escherichia coli*: functional importance of the transmembrane regions of membrane-located protein kinase, EnvZ. J. Biochem. (Tokyo) **111**, 707–713
16 Tokishita, S. and Mizuno, T. (1994) Transmembrane signal transduction by the *Escherichia coli* osmotic sensor, EnvZ: intermolecular complementation of transmembrane signalling. Mol. Microbiol. **13**, 435–444
17 Jung, K., Hamann, K. and Revermann, A. (2001) K^+ stimulates specifically the autokinase activity of purified and reconstituted EnvZ of *Escherichia coli*. J. Biol. Chem. **276**, 40896–40902
18 Leonardo, M. R. and Forst, S. (1996) Re-examination of the role of the periplasmic domain of EnvZ in sensing of osmolarity signals in *Escherichia coli*. Mol. Microbiol. **22**, 405–413
19 Waukau, J. and Forst, S. (1999) Identification of a conserved N-terminal sequence involved in transmembrane signal transduction in EnvZ. J. Bacteriol. **181**, 5534–5538
20 Yaku, H. and Mizuno, T. (1997) The membrane-located osmosensory kinase, EnvZ, that contains a leucine zipper-like motif functions as a dimer in *Escherichia coli*. FEBS Lett. **417**, 409–413
21 Lepre, C. A. and Moore, J. M. (1998) Microdrop screening: a rapid method to optimize solvent conditions for NMR spectroscopy of proteins. J. Biomol. NMR **12**, 493–499
22 Egger, L. A. and Inouye, M. (1997) Purification and characterization of the periplasmic domain of EnvZ osmosensor in *Escherichia coli*. Biochem. Biophys. Res. Commun. **231**, 68–72
23 Ouali, M. and King, R. D. (2000) Cascaded multiple classifiers for secondary structure prediction. Protein Sci. **9**, 1162–1176
24 Selden, L. A., Kinosian, H. J., Estes, J. E. and Gershman, L. C. (1994) Influence of the high affinity divalent cation on actin tryptophan fluorescence. Adv. Exp. Med. Biol. **358**, 51–57
25 Gross, M., Lustig, A., Wallimann, T. and Furter, R. (1995) Multiple-state equilibrium unfolding of guanidino kinases. Biochemistry **34**, 10350–10357
26 Haq, S. K., Rasheedi, S. and Khan, R. H. (2002) Characterization of a partially folded intermediate of stem bromelain at low pH. Eur. J. Biochem. **269**, 47–52
27 Pawar, S. A. and Deshpande, V. V. (2000) Characterization of acid-induced unfolding intermediates of glucose/xylose isomerase. Eur. J. Biochem. **267**, 6331–6338
28 Bagby, S., Tong, K. I. and Ikura, M. (2001) Optimization of protein solubility and stability for protein nuclear magnetic resonance. Methods Enzymol. **339**, 20–41
29 Zappacosta, F., Pessi, A., Bianchi, E., Venturini, S., Sollazzo, M., Tramontano, A., Marino, G. and Pucci, P. (1996) Probing the tertiary structure of proteins by limited proteolysis and mass spectrometry: the case of Minibody. Protein Sci. **5**, 802–813
30 Tomomori, C., Tanaka, T., Dutta, R., Park, H., Saha, S. K., Zhu, Y., Ishima, R., Liu, D., Tong, K. I., Kurokawa, H. et al. (1999) Solution structure of the homodimeric core domain of *Escherichia coli* histidine kinase EnvZ. Nat. Struct. Biol. **6**, 729–734
31 Zoetewey, D. L., Tripet, B. P., Kutateladze, T. G., Overduin, M. J., Wood, J. M. and Hodges, R. S. (2003) Solution structure of the C-terminal antiparallel coiled-coil domain from *Escherichia coli* osmosensor ProP. J. Mol. Biol. **334**, 1063–1076
32 Culham, D. E., Tripet, B., Racher, K. I., Voegele, R. T., Hodges, R. S. and Wood, J. M. (2000) The role of the carboxyl terminal α-helical coiled-coil domain in osmosensing by transporter ProP of *Escherichia coli*. J. Mol. Recognit. **13**, 309–322
33 Chervitz, S. A. and Falke, J. J. (1996) Molecular mechanism of transmembrane signaling by the aspartate receptor: a model. Proc. Natl. Acad. Sci. U.S.A. **93**, 2545–2550
34 Ottemann, K. M., Xiao, W., Shin, Y. K. and Koshland, Jr, D. E. (1999) A piston model for transmembrane signaling of the aspartate receptor. Science **285**, 1751–1754
35 Maruyama, I. N., Mikawa, Y. G. and Maruyama, H. I. (1995) A model for transmembrane signalling by the aspartate receptor based on random-cassette mutagenesis and site-directed disulfide cross-linking. J. Mol. Biol. **253**, 530–546
36 Cochran, A. G. and Kim, P. S. (1996) Imitation of *Escherichia coli* aspartate receptor signaling in engineered dimers of the cytoplasmic domain. Science **271**, 1113–1116

Received 1 July 2004/11 August 2004; accepted 9 September 2004
Published as BJ Immediate Publication 9 September 2004, DOI 10.1042/BJ20041125